Accurate Analytical Models of Fluid Friction in Rectangular Microchannels

S. W. Tchikanda, R. H. Nilson and S. K. Griffiths

Fluid/Thermal Modeling Department
Sandia National Laboratories
MS 9950 7011 East Avenue
Livermore, CA 94550 swtchik@sandia.gov

Keywords: Heat pipes, microchannel flow, fluid friction.

ABSTRACT

This paper presents analytical expressions for the normalized mean velocity of a liquid flowing in a rectangular microchannel. For fully developed laminar flow at low *Reynolds* numbers, the governing *Navier Stokes* equations reduce to a balance between the axial pressure gradient and the viscous shear stresses in the cross-sectional plane. The resulting *Poisson* equation is solved numerically on a nonuniform grid using the finite volume method to obtain axial velocity distributions that are averaged over the channel cross section to extract the normalized mean velocities. These numerical results are used to guide the development of analytical solutions that apply in asymptotic limits of fluid depth and contact angle. These asymptotic solutions are then blended analytically to obtain a relatively simple and accurate comprehensive expression for the mean velocity as a function of contact angle and aspect ratio.

1 INTRODUCTION

Liquid flow in microchannels is important to a number of technologies including cooling of microelectronics by heat pipes and capillary pumped loops as well as capillary wetting of channels in molding processes and in chip-based devices for identification of chemical and biological species. Since channel lengths in these applications greatly exceed lateral channel dimensions, such flows can be accurately and efficiently modeled using one dimensional analyses in which the frictional flow resistance is described in terms of a friction coefficient that depends on the channel geometry, the fraction of the channel depth that is filled with liquid, and the wetting angle at the contact between the meniscus and the solid channel walls.

Although a number of previous numerical studies have provided friction coefficients for some subsets of the important parameter range, they generally do not span a wide range of channel aspect ratios and wetting angles and rarely do they provide accurate and comprehensive analytical approximations needed for application by others. Schneider and DeVos [1] analyzed the heat transport capability of axially grooved heat pipes. They presented an approximate model that includes the influence of liquid/vapor interaction and compared their results with the exact solution of DiCola [2]. However, these results are limited to cases in which the fluid depth is large compared to the radius of the meniscus. Suh et al. [3] investigated the flow of liquid and vapor in trapezoidal and sinusoidal grooves, taking into account the effects of variable shear stress at the interface. They modified the Schneider/DeVos [1] relation for the friction in rectangular grooves to obtain approximations for trapezoidal and sinusoidal grooves, but these are accurate only within limited parameter ranges. Thomas et al. [4] presented a semi-analytical solution and a two-point numerical solution for the mean velocity in trapezoidal grooves with shear stress at the liquid-vapor interface. Although comprehensive, the suggested analytical approximations sometimes yield error as large as 30%.

Here we use numerical solutions of the *Navier Stokes* equations to guide the construction of analytical approximations by blending three asymptotic solutions that apply in different ranges of the ratio of channel width to fluid depth. The approximations are easily applied and are accurate within a few percent over the full range of parameters.

2 GOVERNING EQUATIONS

Capillary flow of an incompressible *Newtonian* liquid is considered for the rectangular groove shown in Figure 1. These straight sided channels are particularly important in heat transfer applications because high-aspect-ratio channels having parallel walls can readily be fabricated from high-conductivity metals using lithographic and electrodeposition processes. As appropriate for sub-millimeter channel widths, the free surface between the liquid and the vapor is assumed to have a constant curvature and hence, a shape given by

$$y = H + \frac{W}{2}\tan\alpha - \sqrt{\frac{W^2}{4\cos^2\alpha} - x^2}. \qquad (1)$$

For fully developed laminar flow at low *Reynolds* numbers, the governing *Navier Stokes* equations reduce to a balance between the axial pressure gradient and the

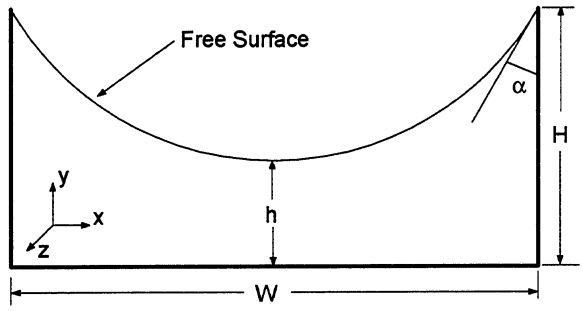

Figure 1: Rectangular groove geometry and coordinate system.

viscous shear stresses in the cross-sectional plane. Thus,

$$\frac{\partial^2 u}{\partial x^2} + \frac{\partial^2 u}{\partial y^2} = \frac{1}{\mu}\frac{\partial p}{\partial z}, \tag{2}$$

where u is the velocity component in the axial direction, μ is the viscosity of the fluid, and p is the pressure.

On the groove walls, the no-slip condition is imposed,

$$u = 0, \tag{3}$$

while the boundary condition on the liquid/vapor interface is

$$\mu\left(\widehat{n}\cdot\nabla u\right) = \tau, \tag{4}$$

where $\widehat{n}$ is the unit outward normal to the interface and τ is the shear stress.

The momentum equation can be put in dimensionless form by introducing the following dimensionless variables

$$x^* = \frac{x}{W},\ y^* = \frac{y}{h},\ u^* = \frac{-u\mu}{W^2\left(\partial p/\partial z\right)},\ \tau^* = \frac{-\tau}{W\left(\partial p/\partial z\right)}. \tag{5}$$

Using Eqs. (5) the dimensionless form of Eqs. (2) and (4) are given by

$$\frac{\partial^2 u^*}{\partial x^{*2}} + \lambda^2\frac{\partial^2 u^*}{\partial y^{*2}} = -1, \tag{6}$$

and

$$\widehat{n}^*\cdot\nabla u^* = \tau^*, \tag{7}$$

where $\lambda \equiv W/h$ is the aspect ratio.

Because Eqs. (6) and (7) are linear, the solution can be decomposed into a pressure-driven flow solution, u_p^*, that satisfies Eq. (6) with zero shear at the interface and a shear-driven flow solution, u_τ^*, that satisfies *Laplace*'s equation subject to a dimensionless shear boundary condition at the interface. Thus, assuming a uniform shear stress along the liquid/vapor interface, the combined solution can be expressed as,

$$u^* = u_p^* + u_\tau^*\tau^*, \tag{8}$$

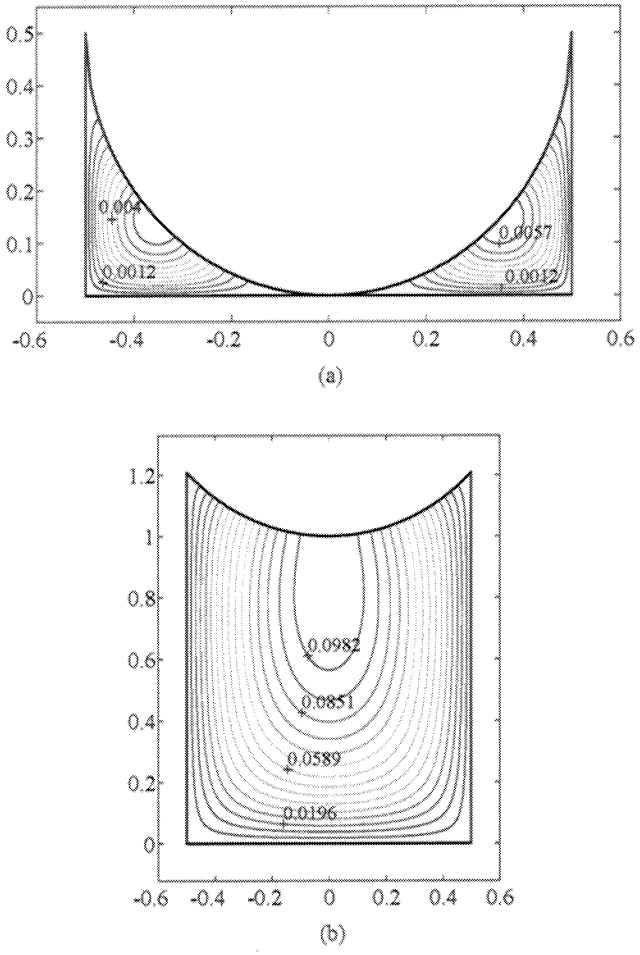

Figure 2: Axial velocity contours for pressure-driven flow: (a) $\alpha = 0^o$, $h = 0$; (b) $\alpha = 45^o$, $h = 1$.

where u_τ^* is driven by a unity shear stress at the liquid/vapor interface.

The governing equations were solved numerically to obtain axial velocity distributions like those shown in Figure 2 for different aspect ratios and contact angles. This was accomplished by discretizing the governing equations on nonuniform grids using the finite volume method. These profiles are then averaged over the channel cross section to obtain the normalized mean velocities,

$$U^* = \frac{1}{A}\iint_A u^*\left(x^*, y^*\right) dA. \tag{9}$$

3 RESULTS FOR PRESSURE-DRIVEN FLOW

Figure 3a shows the mean velocity as a function of aspect ratio for several choices of the contact angle. As λ approaches zero, all the curves collapse onto a single well-known asymptote, $U^* = 1/12$. In the opposite extreme of large λ, all of the curves follow the intermedi-

ate asymptote, $U^* = 1/3\lambda^2$, until turning onto separate horizontal asymptotes, $U_C^*(\alpha)$, describing *corner flows* like that shown in Figure 2a. We note from Figure 1, that these *corner flows* are obtained when $h = 0$ and hence $\lambda = \infty$. For convenience, an alternate aspect ratio is defined as

$$\Lambda = \frac{W}{H} = \frac{2\cos\alpha}{1-\sin\alpha}, \ (h = 0). \tag{10}$$

As seen in Figure 3b, if the mean velocities of these limiting *corner flows* are expressed in terms of Λ instead of α, then they may also be viewed as a transition between asymptotes $U_C^* = 0.0027$ and $U_C^* = 1/7\Lambda^2$ that apply in the limits of small ($\alpha \longrightarrow 0^o$) and large ($\alpha \longrightarrow 90^o$) Λ, respectively. All these asymptotic solutions are blended analytically to obtain a relatively simple and accurate comprehensive expression for the mean velocity as a function of contact angle and aspect ratio. The blend is obtained using the following expression:

$$U^* = \left[\frac{(U_1^* U_2^*)^m}{(U_1^*)^m + (U_2^*)^m}\right]^{1/m}. \tag{11}$$

For the *corner flow* solutions, the asymptotes U_1^* and U_2^* are defined by

$$U_1^* = U_{C,0}^* = 0.0027, \ U_2^* = \frac{1}{7(\Lambda-2)^2 + b(\Lambda-2)^k}, \tag{12}$$

which lead to

$$U_C^* = \left\{\frac{(U_{C,0}^*)^m}{1 + \left(U_{C,0}^*\right)^m \left[7(\Lambda-2)^2 + b(\Lambda-2)^k\right]^m}\right\}^{1/m}, \tag{13}$$

where $U_{C,0}^*$ is the mean velocity when $\Lambda = 2$ ($\alpha = 0$). Eq. (13) is accurate to within 2% relative error with the parameters m, b, and k set to 1.88, 150, and 0.87, respectively.

To obtain a comprehensive expression of the mean velocity for all contact angles and aspect ratios, the asymptotes U_1^* and U_2^* are chosen as

$$U_1^* = \frac{1}{12}, \ U_2^* = \left[\left(\frac{1}{a\lambda + 3\lambda^2}\right)^n + (U_C^*)^n\right]^{1/n}. \tag{14}$$

When Eqs. (14) are substituted into Eq. (11) with the parameters $m = 1.31$, $n = 0.82$, and $a = 8.37$, the mean velocity can be approximated with a maximum relative error of 10% for α in the range $0^o \leq \alpha \leq 60^o$. Different sets of (m, n, a) can be used to obtain different levels of accuracy over various ranges of the contact angle. For the most familiar case of a relatively wide channel having flat interface over most of the channel width, or equivalently for narrow channels with $\alpha \approx 90^o$, the parameters

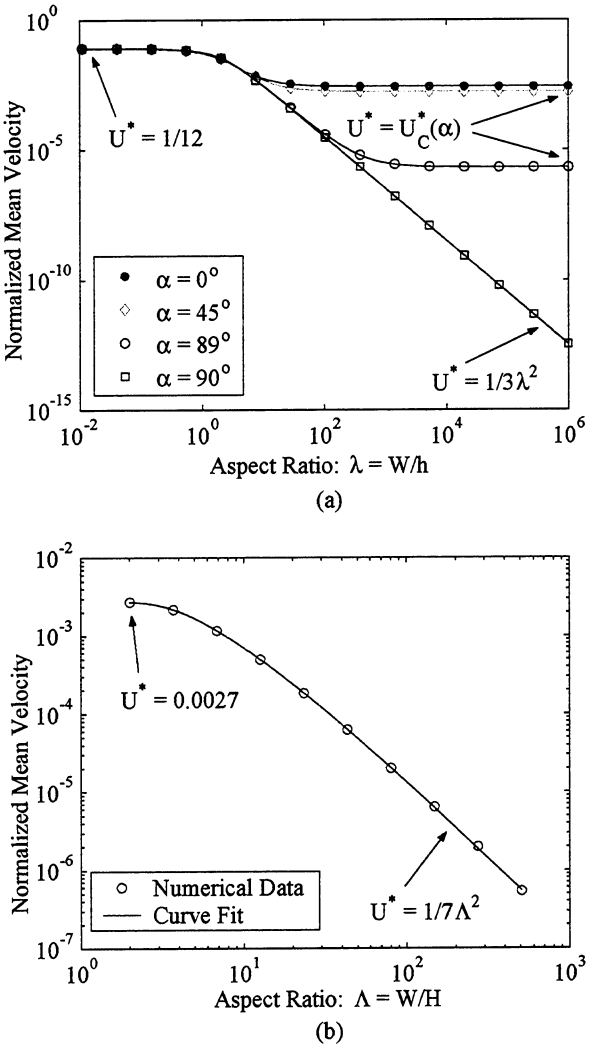

Figure 3: Normalized mean velocity as a function of aspect ratio for the pressure-driven flow: (a) solutions at different contact angles, (b) corner flow solutions.

$m = 1$, $n = 1$,and $a = 2.6$ yield an accuracy of 2.5%. In heat pipe and other capillary pumping applications where small contact angles are of great importance, the parameters $m = 1.4$, $n = 0.83$, and $a = 9.71$ yield a maximum relative error of only 6% for contact angles in the range $0^o \leq \alpha \leq 30^o$.

4 RESULTS FOR SHEAR-DRIVEN FLOW

Figure 4a shows the mean velocity as a function of aspect ratio for several choices of the contact angle for the shear-driven flow. As in the pressure-driven flow, several asymptotes are can be identified and similar blends can be constructed for the mean velocities. The *corner flow* solutions shown in Figure 4b are obtained by sub-

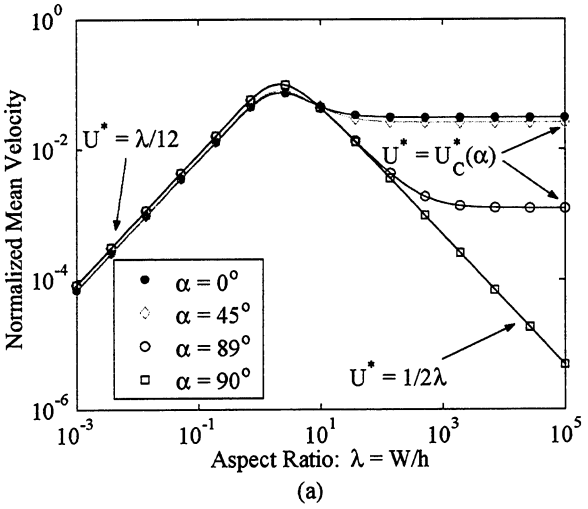

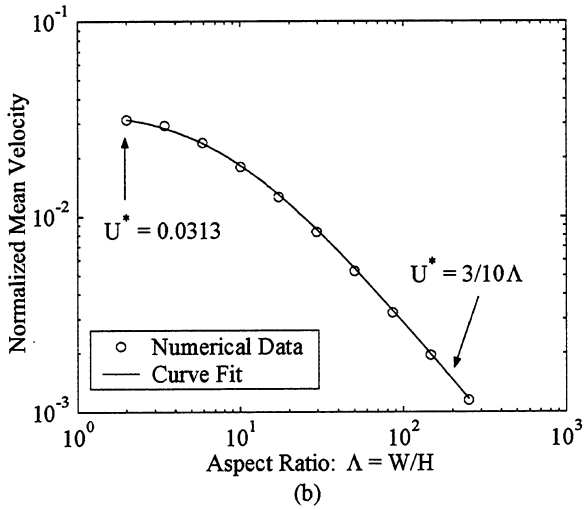

Figure 4: Normalized mean velocity as a function of aspect ratio for the shear-driven flow: (a) solutions at different contact angles, (b) corner flow solutions.

stituting the asymptotes

$$U_1^* = U_{C,0}^* = 0.0313, U_2^* = \frac{3}{10\,(\Lambda - 2)} \qquad (15)$$

into Eq. (11). Thus,

$$U_C^* = \left\{ \frac{\left(U_{C,0}^*\right)^m}{1 + \left(U_{C,0}^*\right)^m \left[\frac{10}{3}\,(\Lambda - 2)\right]^m} \right\}^{1/m}. \qquad (16)$$

When the parameter $m = 1.11$, Eq (16) approximates the mean velocities of the shear-driven *corner flow* to within 4% relative error.

Similar to Eqs. (14), two asymptotes are developed to obtain a comprehensive expression of the mean velocity for all contact angles and aspect ratios:

$$U_1^* = \frac{\lambda}{c},\; U_2^* = \left[\left(\frac{1}{2\lambda + d\lambda^k} \right)^n + \left(U_C^*\right)^n \right]^{1/n}. \qquad (17)$$

The coefficient c is a function of α and given by

$$c(\alpha) = -1.55\alpha^2 + 0.84\alpha + 14.57,\; 0 \le \alpha \le \pi/2. \qquad (18)$$

When Eqs. (17) are substituted into Eq. (11) with the parameters $m = 1$, $n = 1.75$, $d = 1$, and $k = 0.6$ the mean velocity can be approximated with a maximum relative error of 15% for α in the range $0^o \le \alpha \le 90^o$. For contact angles in the range $85^o \le \alpha \le 90^o$ the parameters $m = 2.6$, $n = 1.4$, $d = 5.9$, and $k = -0.3$ yield an accuracy of 5%. For contact angles in the range $0^o \le \alpha \le 30^o$ the parameters $m = 1.1$, $n = 1.38$, $d = 2$, and $k = 0.9$ yield a maximum relative error of only 5%.

5 CONCLUSIONS

In this work the mean velocity of a liquid flowing in rectangular microchannels has been investigated. Both pressure-driven and shear-driven flows have been considered. Accurate analytical expressions for the mean velocities as functions of contact angle and aspect ratio were developed. This was accomplished by blending asymptotic solutions that apply in the limits of small and large aspect ratio for all contact angles. The results show that the mean velocities in both cases are strongly dependent on the contact angle and aspect ratio of the channel.

REFERENCES

[1] G. E. Schneider and R. DeVos, "Nondimensional analysis for the heat transport capability of axially-grooved heat pipes including liquid/vapor interaction," *AIAA Paper*, no. 80-0214, 1980.

[2] G. DiCola, "Soluzionne analitica, amezzo della transformata di fourier, di un problema di fusso in un canale rettangolare." Euratom C.C.R. Ispra (Italy), CETIS, 1968.

[3] J. S. Suh, R. Greif, and C. P. Grigoropoulos, "Friction in micro-channel flows of a liquid and vapor in trapezoidal and sinusoidal grooves," *Int. J. Heat Mass Transfer*, vol. 44, pp. 3103–3109, 2001.

[4] S. K. Thomas, R. C. Lykins, and K. L. Yerkes, "Fully developed laminar flow in trapezoidal grooves with shear stress at the liquid-vapor interface," *Int. J. Heat Mass Transfer*, vol. 44, pp. 3397–3412, 2001.